# Supporting information

## Photocatalytic $CO_2$ reduction using a diazabenzacenaphthenium photosensitizer and a Mn catalyst

Kei Kamogawa,[1]* Shintaro Okumura,[2]* Osamu Ishitani[1]*

[1]Department of Chemistry, Graduate School of Advanced Science and Engineering, Hiroshima University, 1-3-1 Kagamiyama, Higashi-Hiroshima, Hiroshima 739-8526, Japan.

[2]Department of Synthetic Chemistry and Biological Chemistry, Kyoto University, Katsura, Kyoto 615-8510, Japan

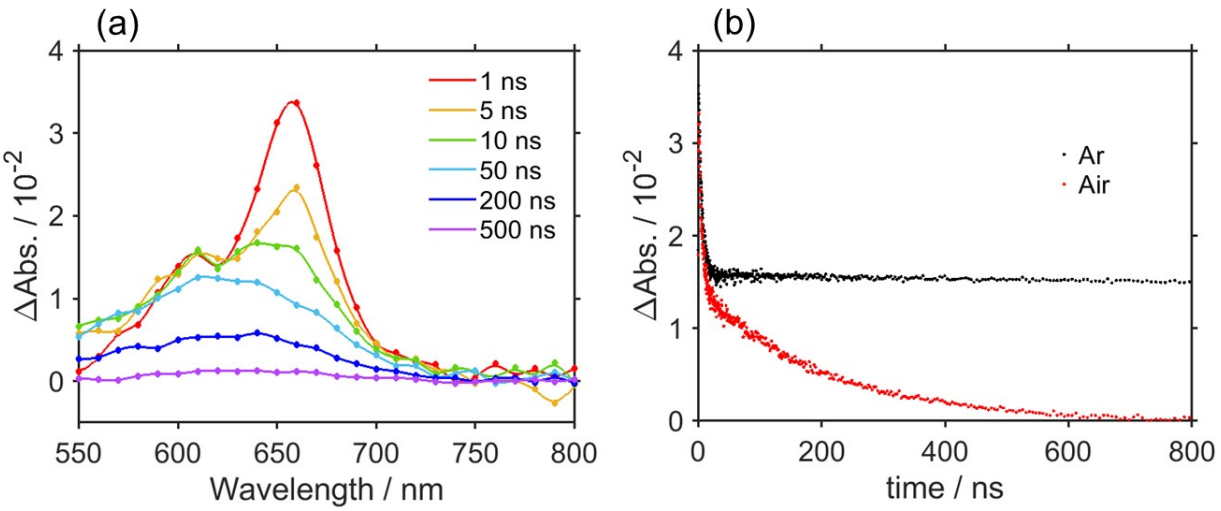


**Figure S1.** (a) Transient absorption (TA) spectra of an aerated DMSO solution containing ***N*-BAP**$^{+}$ (0.4 mM) and TFE (3.78 M) following pulsed excitation at $\lambda_{ex}$ = 355 nm (100 Hz, 17 μJ pulse$^{-1}$). (b) Kinetic traces at 660 nm for Ar-degassed and non-degassed solutions.

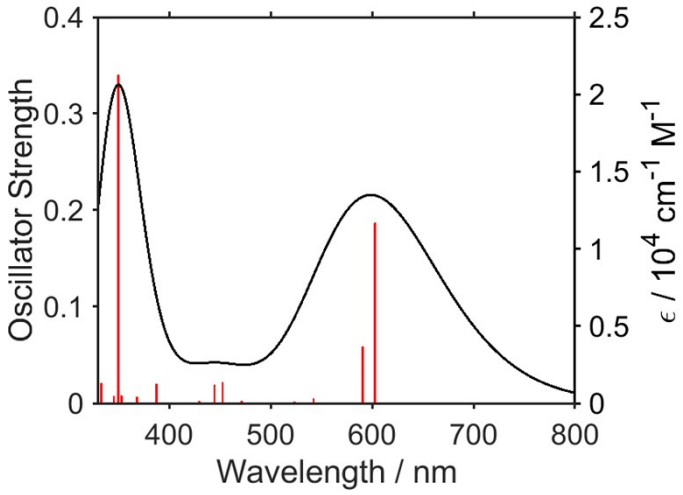


**Figure S2**. TD-DFT-predicted spectrum of $^{3}$***N*-BAP**$^{+}$ in DMSO. FWHM = 2000 cm$^{-1}$.

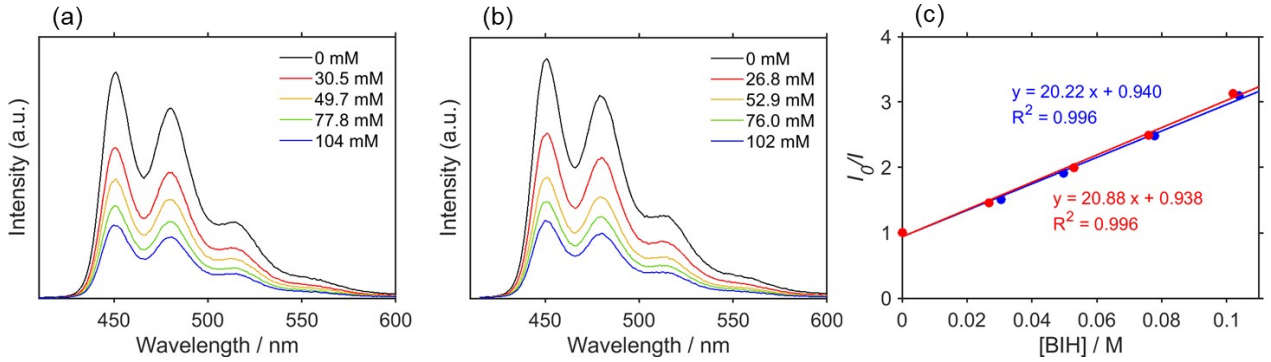


**Figure S3.** Emission spectra of ***N*-BAP**$^+$ measured in DMSO solutions containing BIH and TFE (3.78 M) (a) under air and (b) under Ar. (c) Corresponding Stern–Volmer plots measured under air (blue) and under Ar (red).

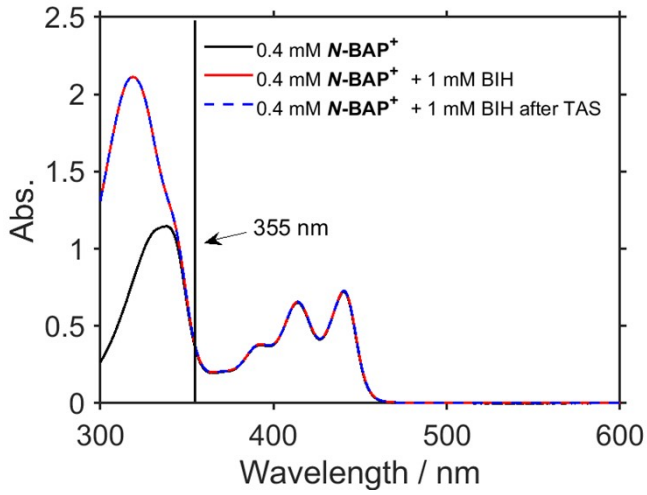


**Figure S4.** UV–Vis absorption spectra of a DMSO-TFE (3.78 M) mixed solution containing ***N*-BAP**$^+$ (0.4 mM), and a DMSO-TFE (3.78 M) mixed solution containing ***N*-BAP**$^+$ (0.4 mM) and BIH (1 mM) before and after TA experiment. Because no change was observed in the sample absorption before and after the TA measurement, the decomposition of ***N*-BAP**$^+$ and variations in BIH concentration during the TA measurements were both negligible. Optical path length: 0.2 cm.

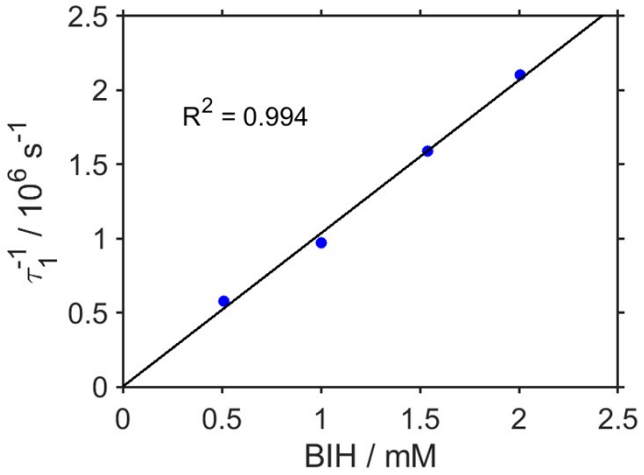


**Figure S5.** Dependence of the lifetime of $^{3}$*$N$-**BAP**$^{+}$ ($\tau_1$) on BIH concentration determined by the global analysis of the TA spectra. From the slope of this plot, the reductive quenching rate constant of $^{3}$*$N$-**BAP**$^{+}$ by BIH was determined to be $1.0 \times 10^{9}$ $M^{-1}$ $s^{-1}$. Ar-purged DMSO solutions containing $N$-**BAP**$^{+}$ (0.4 mM), BIH (0.5–2.0 mM), and TFE (3.78 M) were excited at $\lambda_{ex}$ = 355 nm (50 Hz, 17 μJ $pulse^{-1}$).

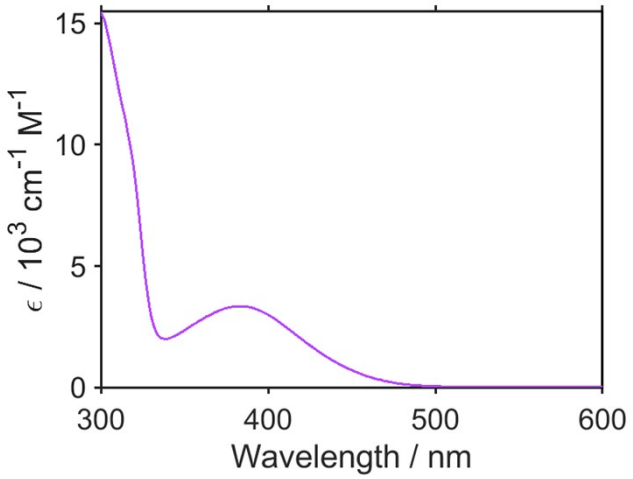


**Figure S6.** UV-Vis absorption spectra of **MnMes** in a $CO_2$-saturated DMSO solution containing TFE (3.78 M) and DIEA (58 mM).

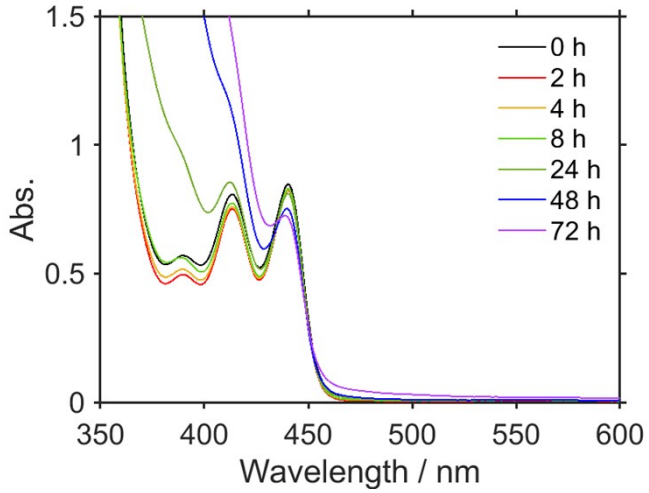


**Figure S7.** UV–Vis absorption spectra of $CO_2$-saturated DMSO solutions containing ***N*-BAP**$^+$ (0.1 mM), **MnMes** (0.05 mM), BIH (0.1 M), TFE (3.78 M), and DIEA (58 mM) after irradiation with 430 nm LED light for the times indicated. These spectra correspond to the solutions used for the photocatalytic reaction shown in Figure 4 of the main text.

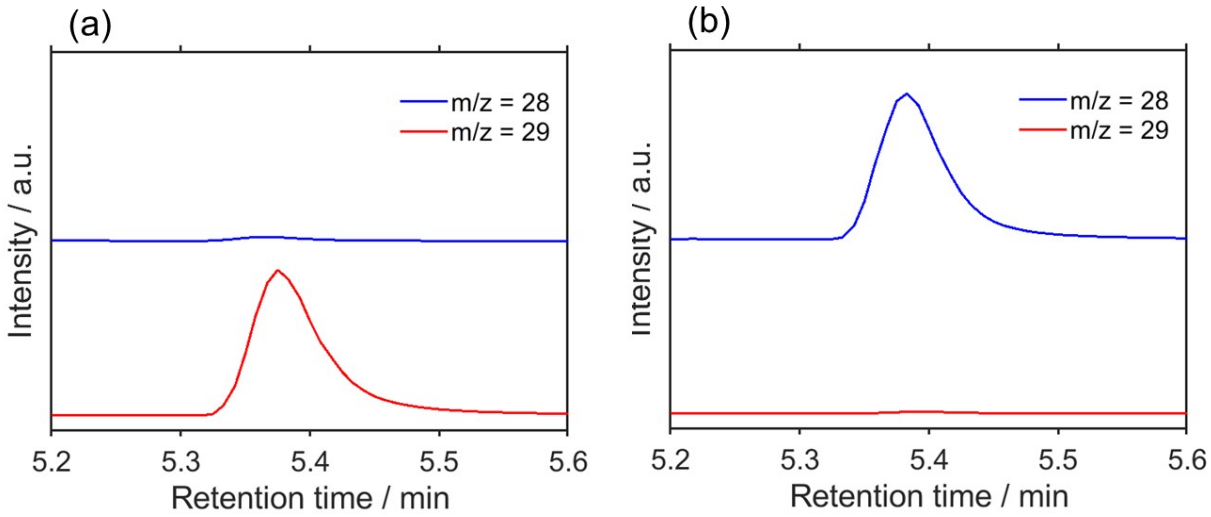


**Figure S8.** GC–MS chromatograms of the gas phase after irradiation. DMSO solutions containing **MnMes** (0.05 mM), ***N*-BAP**$^+$ (0.1 mM), BIH (0.1 M), TFE (3.78 M), and DIEA (58 mM) were irradiated with 430 nm LED light

for 20 h under (a) $^{13}CO_2$ or (b) ordinary $CO_2$.

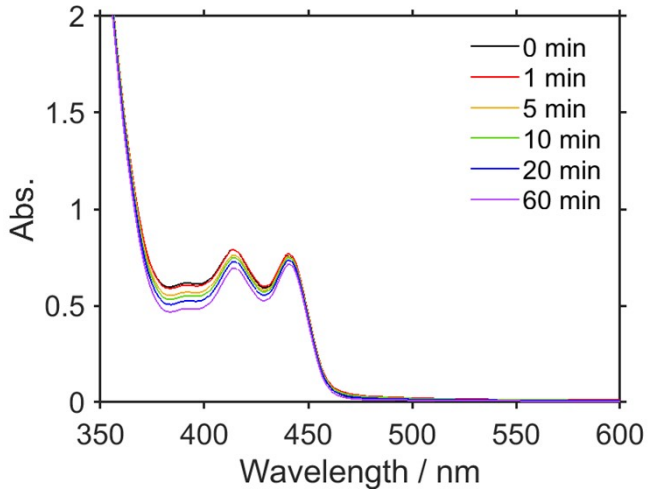


**Figure S9.** UV–Vis absorption spectra of a $CO_2$-saturated DMSO solution containing ***N*-BAP$^+$** (0.1 mM), **MnMes** (0.05 mM), BIH (0.1 M), TFE (3.78 M), and DIEA (58 mM) during the quantum yield measurement. The solution was irradiated with a monochromatic LED light at $\lambda_{max}$ = 430 nm ($5.0 \times 10^{-9}$ Einstein $s^{-1}$).

**Determination of the quantum yield for ISC ($\Phi_{ISC}$)**

$\Phi_{ISC}$ was evaluated by comparing the yield of the triplet excited state between a reference solution containing $[Ru(bpy)_3]Cl_2$, whose ISC quantum yield is close to unity,[1, 2] and the sample solution containing ***N*-BAP**$^+$. Both solutions were irradiated with laser flash at 355 nm (eq. 1).

$$\Phi_{ISC} = \Phi_{ISC,\,Ru} \times \frac{[^{3*}\boldsymbol{N}\text{-}\mathbf{BAP}^+]}{[^3Ru^*]} \times \frac{1 - 10^{-A_{Ru}}}{1 - 10^{-A_{N\text{-}BAP+}}} \qquad (S1)$$

where $\Phi_{ISC,\,Ru}$ ($\approx 1$) is quantum yield of ISC of $[Ru(bpy)_3]Cl_2$, $[3 * \boldsymbol{N}\text{ - }\mathbf{BAP} + ]$ is the concentration of produced triplet excited state of ***N*-BAP**$^+$, $[^3Ru^*]$ is the concentration of produced $^3$MLCT excited state of $[Ru(bpy)_3]^{2+}$, $A_{\boldsymbol{N}\text{-}\mathbf{BAP}}$ and $A_{\mathbf{Ru}}$ are the absorbance at the excitation wavelength (355 nm) of the solutions containing ***N*-BAP**$^+$ or $[Ru(bpy)_3]Cl_2$, respectively.

$[^{3*}\boldsymbol{N}\text{-}\mathbf{BAP}^+]$ was determined using the singlet depletion method reported by Hadley and Keller.[3, 4] In this method, the changes in ΔAbs at both troughs ($\lambda_1$, $\lambda_3$) neighboring a strong singlet peak of ground-state bleaching (GSB) observed in the TA spectrum, and the peak itself ($\lambda_2$), are used to determine the molar absorption coefficient and concentration of $T_1$:

$$\Delta Abs(\lambda_i) = (\varepsilon_T(\lambda_i) - \varepsilon_{S0}(\lambda_i))[T_1]d\,;\ i = 1,2,3 \qquad (S2)$$

where $[T_1]$ is the concentration of the triplet excited state generated by pulsed excitation, $\varepsilon_T$ is the molar absorption coefficient of $T_1$, $\varepsilon_{S0}$ is that of the ground state, and $d$ is the optical path length (0.2 cm). Assuming $\varepsilon_T$ changes linearly in the wavelength range between $\lambda_1$ and $\lambda_3$, eq S3 can be obtained to determine the four unknowns, $\varepsilon_T(\lambda_i)$ (i = 1, 2, 3) and $[T_1]$:

$$\frac{\varepsilon_T(\lambda_1) - \varepsilon_T(\lambda_2)}{\varepsilon_T(\lambda_2) - \varepsilon_T(\lambda_3)} = \frac{\lambda_1 - \lambda_2}{\lambda_2 - \lambda_3} \qquad (S3)$$

Therefore, this method is accurate when the ground-state absorption (Figure 1) is sharply structured and when $T_1$ does not exhibit characteristic absorption in this region. Figure S10 shows the TA spectrum of ***N*-BAP**$^+$ in the region where GSB appears. The maxima and minima of GSB correspond to those of the ground-state absorption, indicating that $^{3*}$***N*-BAP**$^+$ does not exhibit significant absorption in this region. TD-DFT calculations also predict that $^{3*}$***N*-BAP**$^+$ does not show intense absorption here (Figure S2). Therefore, ***N*-BAP**$^+$ satisfies the conditions for accurate application of the singlet depletion method. The concentration of $^{3*}$***N*-BAP**$^+$ generated by laser pulse excitation, $[^{3*}\boldsymbol{N}\text{-}\mathbf{BAP}^+]$, was determined to be 4.5 μM using ΔAbs at $\lambda_2 = 441$ nm and the trough wavelengths $\lambda_1 = 426$ nm and $\lambda_3 = 450$ nm, along with eqs S2 and S3.

Figure S11 shows the temporal change in ΔAbs at 455 nm for an Ar-purged $H_2O$ solution containing 0.1 mM $[Ru(bpy)_3]Cl_2$ after pulsed excitation. From the ΔAbs immediately after excitation (−0.011), the difference molar absorption coefficient of the $^3$MLCT state of $[Ru(bpy)_3]Cl_2$ at 455 nm ($-10{,}100\ M^{-1}\ cm^{-1}$),[5] and the optical path length (0.2 cm), $[^3Ru^*]$ was determined to be 5.5 μM.

By substituting $[^{3*}\boldsymbol{N}\text{-}\mathbf{BAP}^+] = 4.5$ μM, $[^3Ru^*] = 5.5$ μM, and the absorbances at 355 nm ($A_{\mathbf{N\text{-}BAP+}} = 0.328$, $A_{\mathbf{Ru}} =$

0.112) into eq S1, $\Phi_{ISC}$ was calculated to be 57%.

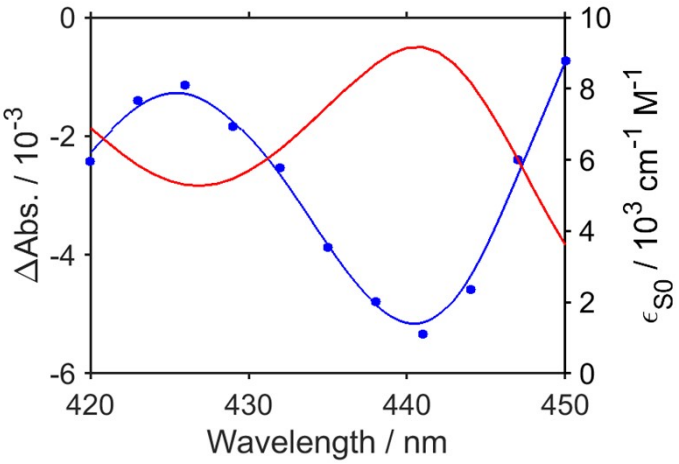


**Figure S10.** (red) Absorption spectrum of ***N*-BAP**$^+$ in DMSO solution containing TFE (3.78 M). (blue) Average TA spectrum of an Ar-purged DMSO solution containing ***N*-BAP**$^+$ (0.2 mM) and TFE (3.78 M) from 100 to 500 ns after pulsed excitation ($\lambda_{ex}$ = 355 nm, 17 μJ pulse$^{-1}$). $A_{\textbf{\textit{N}-BAP}}$ = 0.328. Optical path length: 0.2 cm.

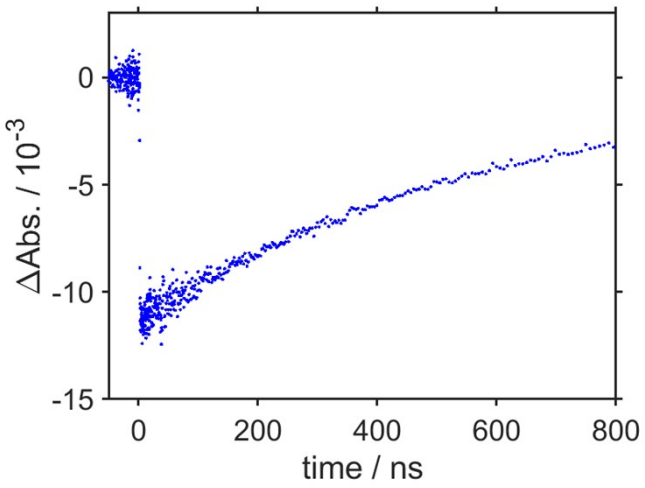


**Figure S11.** Temporal change of ΔAbs at 455 nm of an Ar-purged $H_2O$ solution containing 0.1 mM $[Ru(bpy)_3]Cl_2$ after pulsed excitation ($\lambda_{ex}$ = 355 nm, 17 μJ pulse$^{-1}$). $A_{\textbf{Ru}}$ = 0.112. Optical path length: 0.2 cm.

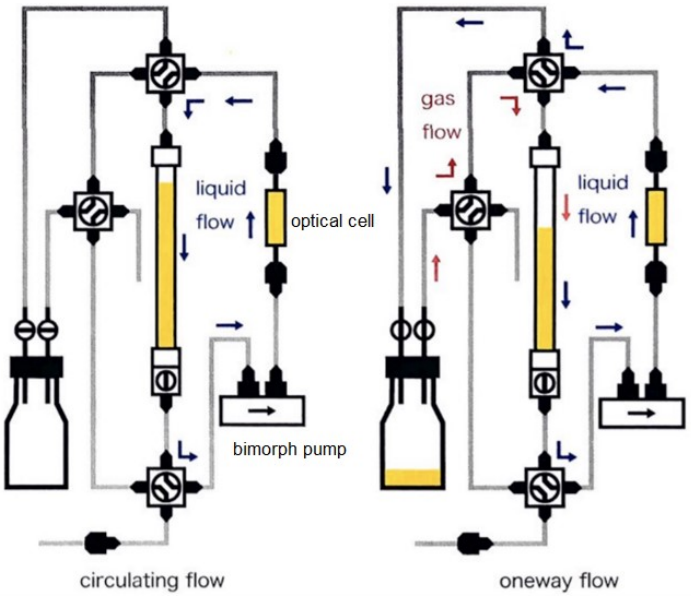


**Figure S12.** Flow cell systems used for the TA measurements.

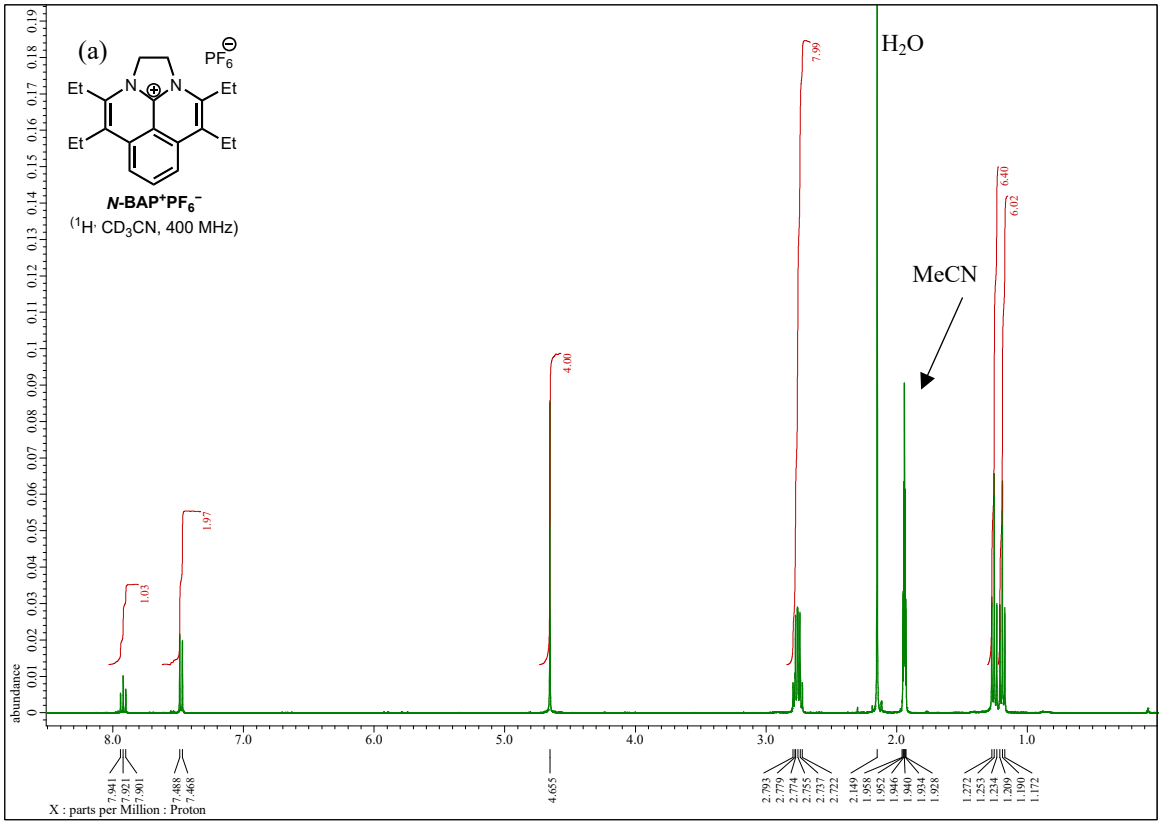

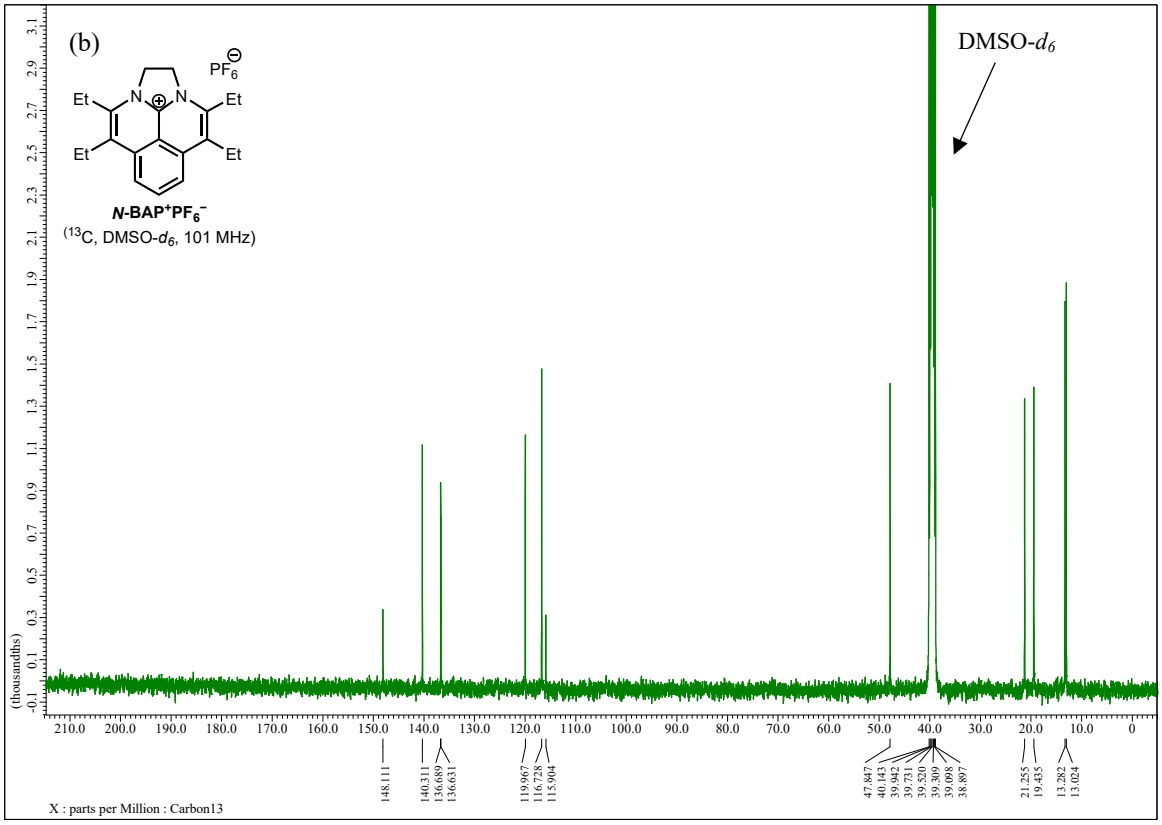


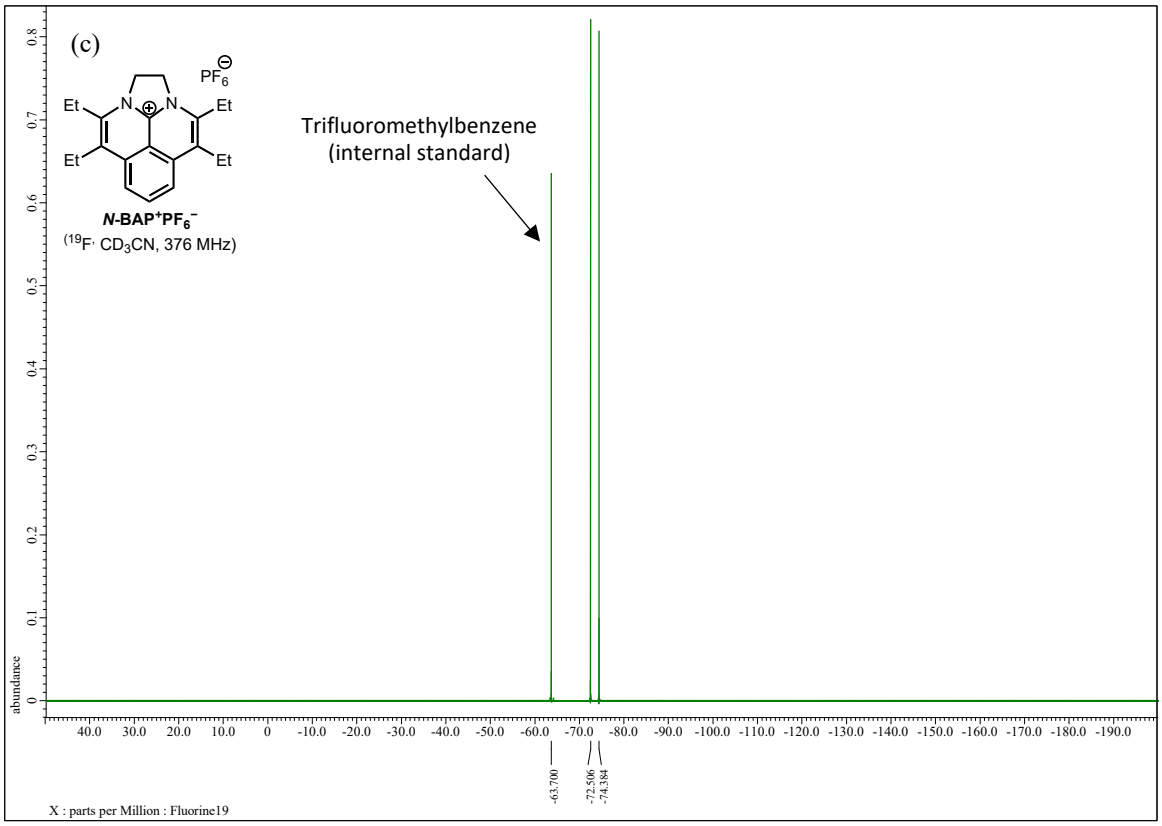


**Figure S13.** NMR spectra of ***N*-BAP$^{+}$PF$_6^{-}$** (a) $^{1}$H, (b) $^{13}$C, (c) $^{19}$F.

1. N. H. Damrauer, G. Cerullo, A. Yeh, T. R. Boussie, C. V. Shank and J. K. McCusker, *Science*, 1997, **275**, 54-57.
2. A. W. Adamson and J. N. Demas, *J. Am. Chem. Soc.*, 1971, **93**, 1800-1801.
3. S. G. Hadley and R. A. Keller, *J. Phys. Chem.*, 1969, **73**, 4351-4355.
4. I. Carmichael and G. L. Hug, *J. Phys. Chem. Ref. Data*, 1986, **15**, 1-250.
5. C. Wang, H. Li, T. H. Bürgin and O. S. Wenger, *Nat. Chem.*, 2024, **16**, 1151-1159.